# NATURAL FREQUENCIES OF ROTATING CANTILEVER FLEXIBLE BEAMS BY USING THE *p*-VERSION OF THE FINITE ELEMENT METHOD

**Hamza cherif S. M.*, Houmat A.***
***Department of Mechanical Engineering , University of Tlemcen, Algeria**

**Keywords**: *gyroscopic effect, stretch deformation, Fourier p-element, rotating beams.*

## Abstract

*A p-version of the finite element method is applied to free vibration analysis of rotating beams in conjunction with the modelling dynamic method using the arc-length stretch deformation. In this study the flexible and the rigid body DOF are supposed uncoupled, the linear equations of motion are derived for flapewise and chordwise bending including the gyroscopic effect. The hybrid displacements are expressed as the combination of the in-plane and out-of-plane shape functions formulated in terms of linear and cubic polynomials functions used generally in FEM plus a variable number of trigonometric shape functions representing the internal DOF. for the rotating flexible beams.*

*The convergence properties of the rotating beam Fourier p-element and the influence of angular speed, boundary conditions and slenderness ratio on the dynamic response are studied. It is shown that by this element the order of the resulting matrices in the FEM is considerably reduced leading to a significant decrease in computational effort.*

## 1 Introduction

Vibration analysis of a rotating cantilever beam is an important subject of study in mechanical engineering. There are many examples in mechanics which can be modelized as rotating cantilever beams, such as turbine blades, turbo-engine blades and helicopter blades. Compared to the beams in the stationary state, the natural frequencies and mode shapes vary significantly with the rotating speed caused by the additional bending stiffness of the beam. Several papers have been presented in the past for modeling the rotating flexible beams, but the first works are attributed to Southwell and Gough [1]. Later, a modest literature has accumulated based on the different analytical method [2-4]. This literature is still being added to as advances in computing and new methods of analysis continue to be developed. The effects of rotary inertia on the natural frequency of beams rotating about the transverse axis were presented by Al-Ansary [5], the free vibration behavior of rotating blades modeled as laminated composites was investigated by Chandiramani, et al [6]. Hu et al [7] used the finite element to study the coupling rigid and flexible body dynamics of rotating beams. To this end, the classical geometrically nonlinear structural model in conjunction with the Cartesian deformation was developed. Centrifugal and Coriolis force field effects are also considered in the formulations, however, serious computational inefficiency results from the non-linearity. Recently a new linear dynamic modeling method was introduced by Yoo et al [8], Chung and Yoo [9]. This method employs the hybrid deformation variables including a stretch variable and Cartesian variables. This method is simpler, more consistent, and more rigorous than the conventional method.

In this study a *p*-version finite element method is applied to free vibration analysis of rotating beams in conjunction with the modeling dynamic method using the arc-length stretch deformation. The linear equations of motion are derived for flapewise and chordwise bending including the gyroscopic effect. The hybrid displacements are expressed as the combination of the in-plane and out-of-plane shape functions formulated in terms of linear and cubic

polynomial functions, used generally in FEM plus a variable number of trigonometric shapes functions [10] representing the internal DOF for the rotating flexible beams. The natural frequency is investigated for the variation of the rotating speed, slenderness ratio and boundaries conditions.

## 2 Governing Equations of Motion

### 2.1 Systems of Co-ordinates

In this section, equations of motion of rotating elastic and isotropic beam, assumed to be initially straight, cantilevered at the based with uniform cross-section $A$, constant length $L$ and mass per unit length $\rho$ are derived. The effects of shear deformations and rotary inertia can be neglected (thickness << length). Figure 1 shows a schematic of a flexible rotating beam. X,Y,Z denotes the inertial frame and $\overline{\mathrm{X}}, \overline{\mathrm{Y}}, \overline{\mathrm{Z}}$ denotes the moving reference frame attached to the beam and rotating about the Z-axis.

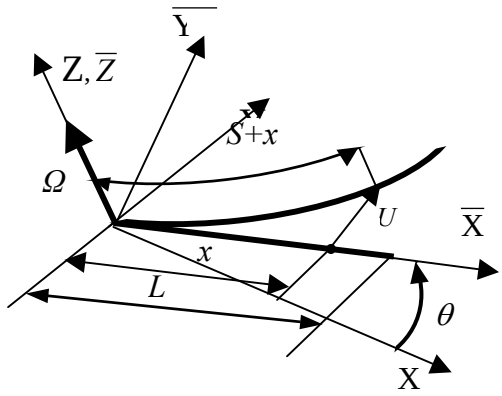


Fig. 1. The Elastic Beam Co-ordinates System.

The position vector $r_p$ of a material point $P$ in the $\overline{\mathrm{X}}, \overline{\mathrm{Y}}, \overline{\mathrm{Z}}$ co-ordinates can be written as

$$r_P = (x+u)\, e_1 + v\, e_2 + w\, e_3 \qquad (1)$$

where $u$, $v$ and $w$ are the components of the elastic deformation $U$ in the moving reference frame co-ordinates.

The inertial frame is related to the beam moving frame by the orthogonal rotation matrix $[A(\theta)]$ and the global position vector $R_p$ is given by

$$R_p = [A(\theta)]\, r_p \qquad (2)$$

where $\theta$ represents the beam rigid body rotation, measured in the X-Y co-ordinates system.

### 2.2 Kinetic and Strain Energy Expressions

In the present study, however a non-Cartesian variable $S$ denoting the arc-length stretch is used instead of $\underline{u}$ witches denotes the Cartesian distance measure of a point $P$ in the axial direction of the undeformed configuration of the beam. The geometric relations between the arc-length stretch $S$ and the Cartesian variables is given by

$$S + x = \int_0^x \sqrt{(1+u_{,\sigma})^2 + (v_{,\sigma})^2 + (w_{,\sigma})^2}\, \mathrm{d}\sigma \qquad (3)$$

Using a binomial expansion of the integrand of equation (3)

$$S = u + \frac{1}{2}\int_0^x (v_{,\sigma})^2\, \mathrm{d}\sigma + \frac{1}{2}\int_0^x (w_{,\sigma})^2\, \mathrm{d}\sigma + H.D.T \qquad (4)$$

The kinetic energy of the beam can be found from

$$T_B = \frac{1}{2}\int_0^L \rho\, \dot{R}_p^{\mathrm{T}} . \dot{R}_p\, \mathrm{d}x \qquad (5)$$

and take the form

$$T_B = \frac{1}{2}\int_0^L \rho\, (a^2 + b^2 + \dot{w}^2)\, \mathrm{d}x \qquad (6)$$

where $a$ and $b$ are given by

$$a = \dot{S} - \int_0^x (\dot{v}_{,\sigma})(v_{,\sigma})\, \mathrm{d}\sigma - \int_0^x (\dot{w}_{,\sigma})(w_{,\sigma})\, \mathrm{d}\sigma - \Omega v \qquad (7)$$

$$b = \dot{v} + \Omega\left(x + S - \frac{1}{2}\int_0^x (v_{,\sigma})^2\, \mathrm{d}\sigma - \frac{1}{2}\int_0^x (w_{,\sigma})^2\, \mathrm{d}\sigma\right) \qquad (8)$$

Based on the Euler-Bernoulli assumptions, the strain energy can be written as

$$U_B = \frac{1}{2}\int_0^x E\,A(S_{,x})^2\,dx + \frac{1}{2}\int_0^x E\,I_y\,(v_{,xx})^2\,dx + \frac{1}{2}\int_0^x E\,I_z\,(w_{,xx})^2\,dx \qquad (9)$$

where the first term in eqn (9) represents the exact stretching energy of the beam.

## 2.3 Beam Fourier *p*-Element Formulation

The rotating flexible beam is descretized into one hierarchical finite element, a Fourier *p*-element is shown in figure2. The element's nodal DOF at each node are $v$, $w$, $v_{,x}$ , $w_{,x}$ and the stretching displacement $S$. The local and non-dimensional co-ordinates are related by

$$\xi = \frac{x}{L} \qquad \text{with } (0 \le \xi \le 1) \qquad (10)$$

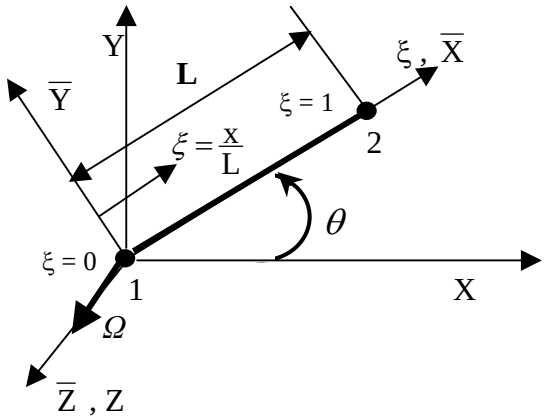


Fig. 2. The Fourier *p*-Element and Co-ordinates.

The vector displacement formed by the hybrid variables $S$, $v$ and $w$ may be expressed as the combination of the in-plane and out-of plane hierarchical shape functions and can be written

$$\begin{cases} S(\xi,t) = \sum_{k=1}^{M_S+2} S_k(t)\, f_k(\xi) \\ v(\xi,t) = \sum_{k=1}^{N_v+4} Y_k(t)\, g_k(\xi) \\ w(\xi,t) = \sum_{k=1}^{N_w+4} Z_k(t)\, g_k(\xi) \end{cases} \qquad (11)$$

and can be expressed as

$$\begin{Bmatrix} S(\xi,t) \\ v(\xi,t) \\ w(\xi,t) \end{Bmatrix} = [\mathrm{N}]\{q\} \qquad (12)$$

where $[\mathrm{N}]$ is the matrix of the shape functions, given by

$$[\mathrm{N}] = \begin{bmatrix} [\mathrm{N}_S] & 0 & 0 \\ 0 & [\mathrm{N}_v] & 0 \\ 0 & 0 & [\mathrm{N}_w] \end{bmatrix} \qquad (13)$$

and

$$[\mathrm{N}_S] = \begin{bmatrix} f_1(\xi)\ f_2(\xi) \ldots f_{M_S+2}(\xi) \end{bmatrix} \qquad (14)$$

$$[\mathrm{N}_{v\,;\,w}] = \begin{bmatrix} g_1(\xi)\ g_2(\xi) \ldots g_{N_{v;w}+4}(\xi) \end{bmatrix} \qquad (15)$$

$M_S$, $N_v$ and $N_w$ are the number of trigonometric shape functions for stretching and bending respectively and $\{q\}$ is the vector of generalized co-ordinates, given by

$$\{q\} = \{S_1,\ldots,S_{M_S+2},Y_1,..,Y_{N_v+4},Z_1,\ldots,Z_{N_w+4}\}^{\mathrm{T}} \qquad (16)$$

The group of the shape functions used in this study is expressed as

$$\begin{cases} f_1(\xi) = 1-\xi \\ f_2(\xi) = \xi \\ f_{r+2}(\xi) = \sin(\delta_r \xi) \end{cases} \qquad (17)$$

and

$$\begin{cases} g_1(\xi) = 1-3\xi^2+2\xi^3 \\ g_2(\xi) = \xi-2\xi^2+\xi^3 \\ g_3(\xi) = 3\xi^2-2\xi^3 \\ g_4(\xi) = -\xi^2-\xi^3 \end{cases} \qquad (18)$$

$$g_{r+4} = \delta_r\,(-\xi + (2+(-1)^r)^2 - (1+(-1)^r\,\xi^3) + \sin(\delta_r \xi)$$

$$\delta_r = r\pi \quad , \quad r = 1, 2, 3, \ldots \qquad (19)$$

The functions ( $f_1$ , $f_2$ , $g_1$ , $g_2$ , $g_3$ , $g_4$ ) are those of the FEM necessary to describe the nodal displacements of the element; whereas the trigonometric functions ($f_{r+2}$, $g_{r+4}$) contribute only to the internal field of displacement and do not affect nodal displacements. The most attractive particularity of the trigonometric functions is that they offer great numerical stability. The beam is modeled by only one element called hierarchical finite element, for irregular geometries more elements can be used.

By applying the Euler-Lagrange equations, the linearized system equations of free vibration of rotating flexible beam can be obtained. The system is a two coupled linear differential equations (eqn (20)) caused by gyroscopic effect, define the chordwise bending vibration and a uncoupled differential equation (eqn(21)) define the flapwise bending vibration.

$$\sum_{m_1=1}^{P_{sv}} (-\omega^2 M^{sv}_{m_1,n_1} + 2\, i\, \omega\, \Omega\, G^{sv}_{m_1,n_1} + K^{sv}_{m_1,n_1} + K^{sv}_{m_1,n_1} + \Omega^2 ( R^{sv}_{m_1,n_1} - M^{sv}_{m_1,n_1}) + \dot{\Omega} G^{sv}_{m_1,n_1} ) q^{sv}_{n_1} = 0, \quad n_1 = 1,2,3,..,P_{sv} \tag{20}$$

$$\sum_{m_2=1}^{P_w} (-\omega^2 M^{w}_{m_2,n_2} + K^{w}_{m_2,n_2} + \Omega^2 R^{w}_{m_2,n_2} ) q^{w}_{n_2} = 0, \quad n_2 = 1,2,3,....,P_w \tag{21}$$

where $i=\sqrt{-1}$ , $\omega$ is the natural frequency, $\dot{\Omega}$ is the rotating acceleration, $q_w$ and $q_{sv}$ are the elements of the vector of generalized co-ordinates. $M_{m,n}$ , $K_{m,n}$ are the coefficients of the conventional hierarchical finite element mass and stiffness matrix, $G_{m,n}$ are the coefficients of the gyroscopic matrix and $R_{m,n}$ are the elements of the additional stiffness matrix caused by the centrifuges effect, where $P_{sv}$ and $P_w$ are the order of the element matrices. The different elements of the matrices are expressed by

$$K^{sv}_{m_1,n_1} = \frac{E\,A}{L} I^{1,1}_{i,j} + \frac{E\,I_z}{L^3} J^{2,2}_{k,l} \tag{22}$$

$$M^{sv}_{m_1,n_1} = \rho\, A\, L\, ( I^{0,0}_{i,j} + J^{0,0}_{k,l} ) \tag{23}$$

$$G^{sv}_{m_1,n_1} = \rho\, A\, L\, ( -IJ^{0,0}_{i,l} + JI^{0,0}_{k,j} ) \tag{24}$$

$$R^{sv}_{m_1,n_1} = \frac{\rho\, A\, L}{2} A^{1,1}_{k,l} \tag{25}$$

$$K^{w}_{m_2,n_2} = \frac{E\,I_y}{L^3} J^{2,2}_{r,s} \tag{26}$$

$$M^{w}_{m_2,n_2} = \rho\, A\, L\, J^{0,0}_{r,s} \tag{27}$$

$$R^{w}_{m_2,n_2} = \frac{\rho\, A\, L}{2} A^{1,1}_{r,s} \tag{28}$$

The coefficients of these matrices are expressed in terms of integrals and are given by

$$I^{\alpha,\beta}_{i,j} = \int_0^1 f_i^{\alpha}(\xi)\, f_j^{\beta}(\xi)\, \mathrm{d}\xi \tag{29}$$

$$J^{\alpha,\beta}_{k,l} = \int_0^1 g_k^{\alpha}(\xi)\, g_l^{\beta}(\xi)\, \mathrm{d}\xi \tag{30}$$

$$JI^{\alpha,\beta}_{k,j} = \int_0^1 g_k^{\alpha}(\xi)\, f_j^{\beta}(\xi)\, \mathrm{d}\xi \tag{31}$$

$$IJ^{\alpha,\beta}_{i,l} = \int_0^1 f_i^{\alpha}(\xi)\, g_l^{\beta}(\xi)\, \mathrm{d}\xi \tag{32}$$

$$A^{\alpha,\beta}_{k,l} = \int_0^1 (1-\xi^2)\, g_k^{\alpha}(\xi)\, g_l^{\beta}(\xi)\, \mathrm{d}\xi \tag{33}$$

Where the vector of generalized co-ordinates are given by

$$\{q^{Sv}\} = \{S_1, S_2, ...., S_{M_S+2}, Y_1, Y_2, ..., Y_{N_V+4}\}^T \tag{34}$$

$$\{q^w\} = \{Z_1, Z_2, Z_3, ..., Z_{N_w+4}\}^T \quad (35)$$

In which the indices $\alpha$ and $\beta$ denote the order of the derivatives. The exact values of the above integrals can easily be found by using symbolic computation [11], which is available through a number of commercial package.

The indices $i$, $j$, $k$, $l$, $r$ and $s$ represent the numbers of hierarchical functions and are defined as

$$\begin{aligned} i; j &= 1,2,...,M_s+2 \\ k; l &= 1,2,...,N_v+4 \\ r; s &= 1,2,...,N_w+4 \end{aligned} \quad (36)$$

the indices $m_1$, $m_2$, $n_1$, $n_2$, are expressed in terms of the indices $i$ , $j$, $k$ , $l$ , $r$ and $s$ as

$$\begin{aligned} m_1 &= i + k \\ n_1 &= j + l \\ m_2 &= r \\ n_2 &= s \end{aligned} \quad (37)$$

where the order $P_{sv}$ and $P_w$ of the element matrices is given by

$$\begin{aligned} P_{sv} &= M_s + N_v + 6, \\ P_w &= N_w + 4 \end{aligned} \quad (38)$$

## 3 Results and Discussions

### 3.1 Convergence study and comparison

In order to see the manner of convergence, the beam is discretized into one element and the number of hierarchical terms is varied. The beam is considered in the stationary state ($\mu$=0) and slender ($\lambda$=70). The frequency parameter and others dimensionless parameters are introduced,

$$\omega^* = \sqrt{\frac{\rho A L^4}{E I}}\,\omega \quad (39)$$

$$\mu = \sqrt{\frac{\rho A L^4}{E I}}\,\Omega \quad (40)$$

$$\lambda = \sqrt{\frac{AL^2}{I}} \quad (41)$$

where $\omega^*$ , $\mu$ and $\lambda$ are respectively the frequency parameter, the angular speed parameter and the slenderness ratio.

Results for the forth lowest bending modes and the two first stretching modes of C-F beam are shown in Table 1 along with exact solutions. The symbolism C-F indicates that the first node is clamped and the second node is free. Table 1 clearly shows that convergence from above to the exact values occurs as the number of trigonometric hierarchical terms is increased and highly accurate solutions are obtained despite the use of a few hierarchical terms, an upper-bound solution to the exact values, and uniform, monotonic convergence is guaranteed.

The performance of the proposed Fourier *p*-element can be verified by comparing the frequency parameter with that of the modal analysis [8] and the finite element method [9] of rotating cantilever flexible beams. Table2 shows that for $\lambda$ = 70 and various values of $\mu$, the results obtained using the present formulation with 30 DOF, these are compared with finite elements formulations, the number of elements used is 100 two nodes beams elements (300 DOF), the trigonometric hierarchical finite element was found to yield a better accuracy with fewer system degrees of freedom. It is observed from these table that the present results are fairly in good agreement with those of the modal analysis (error < 0,02%), excepted for $\mu$ = 50, in the case of chordwise bending vibration, the results from both the HFEM and FEM agree to a remarkable degree; however, some differences are noticed between these sets of results and those of [8].The source of error that can account for this difference is the incomplete convergence in [8]. From the above convergence and comparison studies, a 24 trigonometric shape functions has been employed in the subsequent analysis.

### 3.2 Results

Individual and joint variation of the angular speed and the slenderness ratio is found to influence greatly the chordwise bending natural frequency with and without coupling. In the case of chordwise bending vibration without coupling, figures 2-3 shows how the frequency of the first five bending modes and the first stretching mode of the rotating beam vary with angular speed parameter. The dotted lines in the figures represent the results of ignoring the coupling terms. The bending curves frequency B1-B5 (dotted lines) increase with increasing angular speed parameter. The stretching curves frequency S1-CI (dotted lines) decrease with increasing angular speed parameter and become zero at a specified value of angular speed parameter.

In the second case the coupling effect is considered, the bending curves frequency B2-B5 increase with increasing angular speed parameter, the form of the first and second mode is preserved throughout the range of angular speed considered here, the first bending curves B1 decrease and the stretching curves frequency S1 increase with increasing angular speed.

| $N_v$ ($M_S$) | Bending modes | | | | Stretching modes | |
|---|---|---|---|---|---|---|
| | 1st | 2nd | 3rd | 4th | 1st | 2nd |
| 0 (2) | 3.5327 | 34.8068 | --- | --- | 110.0689 | 333.7549 |
| 4 (6) | 3.1560 | 22.0366 | 61.7316 | 121.7971 | 109.9624 | 330.0538 |
| 8 (10) | 3.1560 | 22.0345 | 61.6990 | 120.9183 | 109.9573 | 329.9108 |
| 12 (14) | 3.1560 | 22.0345 | 61.6974 | 120.9041 | 109.9563 | 329.8837 |
| 16 (18) | 3.1560 | 22.0345 | 61.6972 | 120.9024 | 109.9560 | 329.8751 |
| 20 (22) | 3.1560 | 22.0345 | 61.6972 | 120.9020 | 109.9559 | 329.8717 |
| 24 (26) | 3.1560 | 22.0345 | 61.6972 | 120.9019 | 109.9558 | 329.8693 |
| Exact | 3.1560 | 22.0345 | 61.6972 | 120.9019 | 109.9557 | 329.8672 |

Table 1: Convergence of the lowest frequencies parameters $\omega^*$ of cantilever beam as a function of the number of the trigonometric hierarchical terms for the chordwise motion when $\mu$=0 and $\lambda$=70 .

| $\mu$ | Flapwise | | | Chordwise with coupling | | |
|---|---|---|---|---|---|---|
| | Yoo [8] | Chung [9] | Present analysis | Yoo [8] | Chung [9] | Present analysis |
| 2 | 4,1373 | 4,1373 | 4,1373 | 3,6196 | 3,6196 | 3,6195 |
| 4 | 5,5850 | 5,5850 | 5,5850 | ---- | ---- | 3.8880 |
| 6 | 7,3604 | 7,3604 | 7,3603 | ---- | ---- | 4.2393 |
| 8 | 9,2569 | 9,2568 | 9,2568 | ---- | ---- | 4.6105 |
| 10 | 11,2025 | 11,2023 | 11,2023 | 4.9703 | 4.9700 | 4.9700 |
| 50 | ---- | ---- | 51.0805 | 7.5540 | 7.3337 | 7.3362 |

Table 2: Comparison of the first frequency parameter ω* in flapwise and chorwise bending vibration ( $\lambda$=70 ).

Another interesting phenomenon can be observed in figures 2-3, the first phenomenon is called crossing modes and the second is called veering modes. It is well known that frequency curves only cross when the associated modes of free vibration belong to different symmetry groups, and this in turn leads to are ordering of the modes. Such a crossing is evident in figure 2 involving the fourth bending frequency B4 and the first stretching frequency S1 curves and the mode re-ordering that takes place at such a crossover. The third bending frequency curves B3 and the first stretching curve S1 veer, the mode shapes change abruptly around the veering region.

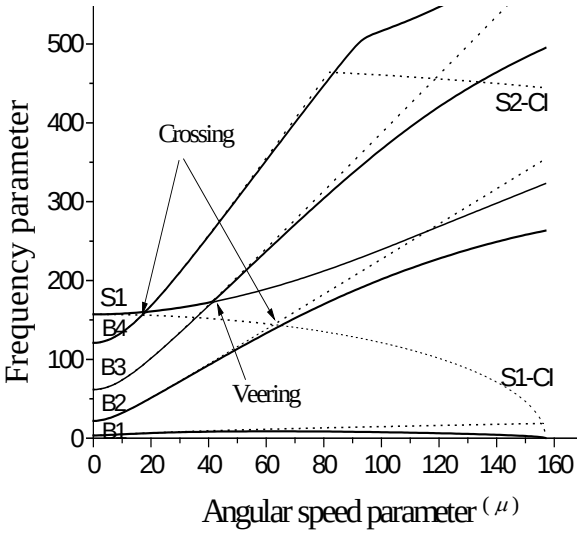


Fig 3: Chordwise bending vibration variations for Cantilever beams with and without coupling ($\lambda$ =100).

After this results, the differences between the two cases are summarized: (i) in the results obtained by ignoring the coupling effect, the first bending frequency increase and the stretching frequency decreases as the angular speed increases. However, this is not true when the coupling effect is included. (ii) the difference between the solid lines and dotted lines remains significant if $\mu$ increase.

Figure 4 gives the trajectory of the lowest frequency parameter for rotating cantilevered beams while varying the slenderness ratio.

When the coupling effect is included, the centrifugal inertia force plays the role to buckle the beam.

The first bending frequency curves decreases and becomes zero at a specific angular speed called buckling speed with increasing angular speed parameter. Variation of the angular speed and the slenderness ratio influence greatly the first bending natural frequency. The buckling speed is influenced directly by the slenderness ratio. The Buckling speed is proportional to the slenderness ratio.

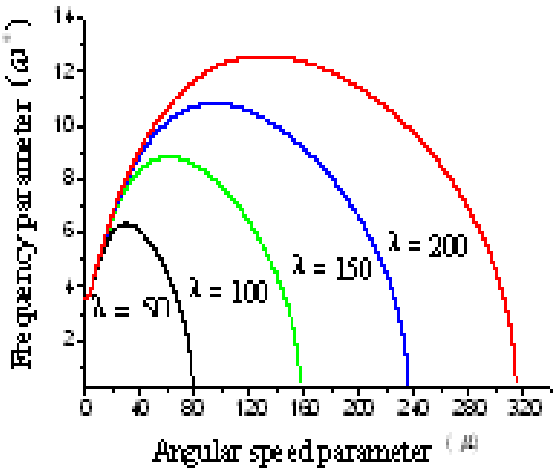


Fig 4 : Chordwise frequency parameter as a function of slenderness ratio ($\lambda$) for cantilever beams.

## Conclusion

The hierarchical finite element method is developed and used to find the natural frequency of free vibration analysis of rotating beams with different boundary conditions in conjunction with the new modeling dynamic method using the arc-length stretch deformation. The main conclusions have emerged from this work these are itemized below: (i) monotonic and uniform convergence is found to occur as the number of hierarchical modes is increased. It is shown that by this element the order of the resulting matrices in the

FEM is considerably reduced leading to a significant decrease in computational effect. (ii) the dynamic characteristics of rotating beams are influenced significantly by varying individually or jointly its angular speed and slenderness ratio. (iii) the difference between the chordwise bending vibration with coupling and without coupling remains significant in the high angular speed region. (v) the case when the gyroscopic effect is considered, the beam buckle at an angular speed called buckling speed, proportional to slenderness ratio.

## References


[1] Southwell and Gough The free transverse vibration of airscrew blades. *British A.R.C.*, *Report and Memoranda*, No. 655, 1921.

[2] Putter S. and Manor H. Natural frequencies of radial rotating beams. *J. Sound Vib*, Vol. 56, pp 175-85, 1967.

[3] Wright A., Smith, C. Thresher R. and Wang J. Vibration modes of centrifugally stiffened beams. *J. of Applied Mechanics*, Vol. 49, pp 197-202, 1971.

[4] Kane T. R., Ryan R. R. and Banerjee A. K. Dynamics of a cantilever beam attached to a moving base, *Journal of Guidance, Control, and Dynamics*, Vol. 10, 139-151, 1987.

[5] Al-Ansary M. D. Flexural vibrations of rotating beams considering inertia, *Computers and structures*, Vol. 69, pp 321-328, 1998.

[6] Chandiramani N. K., Librescu L. and Shete C. D. On the free-vibration of rotating composite beams using a higher-order shear formulation., *J. Aerosp. Sci. Technology*, Vol. 6,8, pp 545-561, 2002.

[7] Hu K., Vlahopoulos N. and Mourelatos Z. P. A finite element formulation for coupling rigid and flexible body dynamics of rotating beams., *J. Sound Vib.*, Vol. 253,1, pp 903-630, 2002.

[8] Yoo H., Ryan R. and Shin S. H. Vibration analysis of rotating cantilever beams, *J. Sound Vib.*, Vol. 212,5, 807-828, 1998.

[9] Chung J. and Yoo H. H. Dynamic analysis of a rotating cantilever beams by using the finite element method, *J. Sound Vib.* , Vol. 249,1, pp 147-164, 2002.

[10] Houmat A. A sector Fourier *p*-element applied to free vibration analysis of sectorial plates, *J. Sound Vib.*, Vol. 243,2, pp 269-282, 2001.

[11] Bardell N. S. The application of symbolic computing to hierarchical finite element method, *Int. J. num. Meth. Engng.*, Vol. 28, pp 1181-204, 1989.